Blood First Edition Paper, prepublished online September 1, 2017; DOI 10.1182/blood-2016-10-740241

Manuscript Title: Eltrombopag: a powerful chelator of cellular or extracellular iron(III) alone or combined with a second chelator

Running Title: The role of Eltrombopag in iron chelation

Authors:

Evangelia Vlachodimitropoulou[a], Yu-Lin Chen[b], Maciej Garbowski[a], Pimpisid Koonyosying[a], Bethan Psaila[c], Martha Sola-Visner[d], Nichola Cooper[c], Robert Hider[b], John Porter[a]

[a] Haematology Department, Universtiy College London

[b] Institute of Pharmaceutical Science, King's College London

[c] Haematology Department, Hammersmith Hospital, Imperial College London

[d] Paediatrics Department, Boston Children's Hospital

Email:
evangelia.koumoutsea.11@ucl.ac.uk
yu-lin.chen@kcl.ac.uk
maciej.garbowski@ucl.ac.uk
pimpisid_m@hotmail.com
b.psaila@imperial.ac.uk
martha.sola-visner@childrens.harvard.edu
nicholacooper@yahoo.com
robert.hider@kcl.ac.uk
j.porter@ucl.ac.uk

Abstract word count: 193

Manuscript word count: 4000

Figures: 5 (+1 supplementary)

Tables: 3

References: 56

Abstract

Eltrombopag (ELT) is a thrombopoietin receptor agonist, also reported to decrease labile iron in leukemia cells. Here we examine the previously undescribed iron(III)-coordinating and cellular iron-mobilizing properties of ELT. We find a high binding constant for iron(III) (log β_2=35). Clinically achievable concentrations (1μM) progressively mobilised cellular iron from hepatocyte, cardiomyocyte and pancreatic cell lines, rapidly decreasing intracellular ROS and also restoring insulin secretion in pancreatic cells. Decrements in cellular ferritin paraleled total cellular iron removal, particularly in hepatocytes. Iron mobilisation from cardiomyocytes exceeded that obtained with deferiprone, desferrioxamine or deferasirox at similar iron-binding equivalents. When combined with these chelators, ELT enhanced cellular iron mobilisation, this being greater than additive (synergistic) with deferasirox. Iron-binding speciation plots are consistent with ELT donating iron to deferasirox at clinically relevant concentrations. ELT scavenges iron citrate species faster than deferasirox, but rapidly donates the chelated iron to deferasirox, consistent with a shuttling mechanism. Shuttling is also suggested by enhanced cellular iron mobilisation by ELT when combined with the otherwise ineffective extracellular hydroxypyridinone chelator, CP40. We conclude that ELT is a powerful iron chelator that decreases cellular iron and further enhances iron mobilisation when combined with clinically available chelators.

Key points

- Eltrombopag is a powerful iron chelator, mobilising iron, ferritin, reducing ROS and restoring insulin production at clinically achievable levels.
- Eltrombopag enhances cellular iron chelation when combined with clinically available iron chelators through the shuttling of iron(III).

Keywords

Iron overload; Iron chelation; Eltrombopag; Insulin

INTRODUCTION

Eltrombopag (ELT) is an orally bioavailable small molecular thrombopoietin receptor (TPO-R) agonist, approved for the treatment of Idiopathic Thrombocytopenia (ITP) and thrombocytopenia associated with chronic hepatitis C. An under-appreciated property of ELT is its binding to metal ions and in particular to iron(III). Oral consumption of ELT with calcium-, aluminium-, and magnesium-containing foods reduced absorption of these metals [1, 2] and this could be due to chelation of metal ions [1]. ELT also decreased labile iron within leukemia cells[3] which could be relevant to its antiproliferative and apoptotic effects in acute myeloid leukemia[3, 4], as well as the treatment of hepatocellular carcinoma[5]. In principle, some beneficial effects on hematopoiesis in myelodysplastic syndrome (MDS)[6] and aplastic anemia[7, 8] could also derive from iron chelation. Our preliminary findings suggested that low ELT concentrations could mobilise cellular iron[9, 10]. ELT might therefore have a role to treat iron overload conditions, either alone or when combined with clinically licensed chelators. However, little is known about the iron-binding properties of ELT. Unknowns include the iron-coordination mechanism, iron(III)-binding constant, effects on iron-induced reactive oxygen species (ROS), effects on storage iron, relative interaction with different cell types, and mechanisms of interaction with other chelators.

Iron chelation therapy is used to treat transfusional iron overload in thalassemias, sickle cell disease and MDS. Non-transfusional iron overload may also be treated with iron chelation. While three iron chelators are now licensed, the removal of excess iron is slow and treatment can also be limited by chelator toxicity, particularly at higher doses. Therefore combinations of chelators have been used to enhance chelation. While simply additive effects can be valuable, true synergism, where one chelator increases the rate of access of a second chelator to iron pools, would be valuable[11].

The ability of an iron chelator to mobilize cellular iron is related to the iron-binding constant and the ability of the iron chelator to enter cells[11]. Thus, chelators with low lipid solubility, or large molecular weight, enter cells slowly and have little effect on iron release[12]. These same properties also affect iron release in animal models[13], as well as affecting their access to intracellular iron pools[14], including metalloenzymes[15, 16], cell cycle, growth[17] and apoptosis[18]. The two largest chelateable iron pools are, firstly, within hepatocytes where over 70% of body iron is deposited and, secondly, iron released from macrophages after catabolism of red

cells[19]. The most rapidly chelateable iron pool within cells is the so-called labile iron pool (LIP), which is relatively small at any moment and is predominantly contributed to by intracellular ferritin catabolism[19, 20].

In this paper we have investigated the iron-binding properties of ELT, its ability to mobilize intracellular iron and to decrease ROS-mediated cellular damage, using a recently described cell culture model[11]. Chelators can be metabolically inactivated at their iron-binding sites, particularly in hepatocytes, but with wide interspecies variability, and where metabolism in rodents, and hence chelator efficacy, can differ significantly from humans[21, 22]. *In vitro* screening therefore ideally needs to include human-derived cells. We have included a human hepatoma cell (HuH7) as the primary screen, as drug metabolism is well described and has the advantage of stability in culture, whereas primary cells can lose key metabolism enzymes within hours of isolation. Iron overload in myocardium and endocrine system is quantitatively much smaller than in the liver, but damage is clinically important, causing fatal cardiomyopathy and type-I diabetes, respectively. We have therefore also investigated cell lines derived from these cells. Decrements in total cellular iron and ferritin induced by ELT, have been compared with clinically licensed chelators. We have also examined whether ELT diminishes iron-induced intracellular ROS and thereby restores cell function. We have investigated whether additional iron chelation can be achieved by combining ELT with other chelators, and examined the mechanisms by which this occurs.

MATERIALS AND METHODS

Spectrophotometric method for pK_a and iron stability constant

An automated titration system[20] was utilized under the conditions of constant temperature at 25°C and constant ionic strength at 0.1M, using 0.1M KCl, 0.1M HCl and 0.1M KOH. The pH electrodes were calibrated using the GLEE program[23]. The titration data were analysed using the pHab program[24]. Species plots were calculated using the HYSS program[25]. Analytical grade reagent materials were used in all solutions.

Determination of kinetics of iron binding to ELT, DFX and CP40.

These were performed spectrophotometrically, using difference spectra where necessary, with a Varioscan Flash plate reader (UK). Kinetic data were plotted using absorbance for ELT or DFX_2Fe complexes. Wavelengths chosen for kinetic analysis were determined from

spectral plots of ELT, DFX, and their respective iron complexes. Buffered ferric citrate was prepared[26] using concentrated MOPS pH 7.4. Eltrombopag was prepared as a 1% solution in DMSO. ELT-iron complexes were prepared as follows: ELT/DMSO aliquot was mixed with ferric chloride atomic standard solution added at desired molar ratios. pH was increased by adding 1M MOPS pH 7.4. Deferasirox 1% solution was prepared in DMSO. ELT in culture media was diluted to ensure final concentration of DMSO <1%.

The cellular models and iron measurements

The human hepatocarcinoma (HuH7) and rat cardiomyocyte (H9C2) cell lines were purchased from Sigma-Aldrich UK. RINm5F rat pancreatic cell line, which secretes insulin following a glucose challenge, was from LGC ATCC Sales, UK. H9C2 and HuH7 cells were plated, cultured and iron-loaded as recently described[9, 11]. Iron loading was obtained by serially treating cells with 10% Fetal Bovine Serum (FBS)-RPMI media over two ten-hour periods. Increments in cellular iron differed between cell types (threefold in HuH7: a twofold in H9C2 and fourfold in RINm5F cells). Cell washing, chelator exposure and measurement of cellular iron using ferrozine assay, adjusted for cellular protein, was as described[11]. Iron release was performed in serum-free medium, as FBS contained free iron that bound chelators extracellularly, decreasing efficacy. Reports of ELT inhibition by serum[4] are more likely a consequence of iron contamination in FBS than protein binding to ELT *(see supplementary data).*

Cell damage and viability, utilized the 'LDH Cytotoxicity Detection Kit' (Takara Bio Inc). Human and rat tissue ferritin of cell lysates were measured by enzyme-linked immunosorbent assay (ELISA) kits (Cusabio, Wuhan, China and My BioSource, San Diego, USA respectively). Desferrioxamine (DFO), Deferiprone (DFP) and Deferasirox (DFX) were purchased from Sigma-Aldrich, UK and ELT from Generon, UK.

Detection of Reactive Oxygen Species

A cell-permeable oxidation-sensitive fluorescent probe 5,6-carboxy-2',7'-dichlorofluoresceindiacetate (DCFH-DA) (Molecular Probes, Leiden, Netherlands) was used, where non-fluorescent DCFH-DA is hydrolyzed to DCFH inside of cells, yielding highly fluorescent DCF in the presence of intracellular hydrogen peroxide (H_2O_2). Cells plated in Corning 24-well plates (Sigma-Aldrich, MA, USA) were pre-incubated with 4mM HDCF-DA for 30 minutes at 37°C. Chelators were then added, and fluorescence recorded

continuously over 90 minutes (excitation at 504nm, emission at 526nm). The time between the addition of chelators and commencing ROS recording was 3-5 minutes.

Insulin quantification

Following iron loading and chelator treatment, the cells were challenged with Krebs' Ringer Buffer twice, for one hour at a time, containing 2.8mM and 16.7mM glucose[27, 28]. The supernatant was then collected and insulin concentration determined using a standard rat insulin ELISA kit (Life Technologies Limited, UK).

RESULTS

Iron(III)-binding and speciation plots for ELT alone or combined with other chelators

The previously undescribed iron(III)-binding properties of ELT are key to understanding the effect on cellular iron mobilisation, either alone or when combined with other chelators. The iron-binding properties of ELT in **Figure 1** and **Table 1** were determined specifically for this communication. The log P value of ELT was derived from a computer program[29]. The usual chemical representation of ELT is shown in structure **1**, lacking a high affinity iron(III)-binding site (**Figure 1A)**. However ELT can be represented as a mixture of two tautomers; the second (**2)** possessing a potential tridentate iron(III)-binding site. The 1:1 complex (**3**) possesses zero net charge (**Table 1**) and has a molecular weight <500, similar to the DFP-iron complex. The speciation plot for iron(III)/ELT (**Figure 1B**) indicates a mixture of the 1:1 and 2:1 complexes at pH 7.4. **Figure 1 (C, D, E)** shows speciation plots of iron(III) (1μM) binding at increasing concentrations of ELT (1-10μM) in the presence of DFO 1μM, DFP 3μM and DFX 2μM. These predict proportions of iron bound to ELT or a second chelator, after reactions have proceeded to completion. Thus, for example, at 1μM ELT over 99% of iron(III) will be bound to DFO (**A**), whereas about half of the iron will be bound to DFP (**B**) and about 70% to DFX (**C**). These values are helpful in interpreting iron-release studies using combinations of ELT with a second chelator but do not predict the rates at which reactions proceed.

ELT decreases cellular iron in cardiomyocyte and hepatocyte cell lines

Mobilisation of total cellular iron from HuH7 cells was examined between 1 and 30μM ELT at 8h (**Figure 2A**). These are clinically relevant as C_{max} plasma concentrations of 8, 18, and 28μM, have been reported at 30, 50, and 75 mg/day[30]. In cardiomyocytes, as little as 1μM ELT achieved significant mobilisation after only 1 hour (**Figure 2B**). A 2:1 binding of ELT to iron(III) (**Figure 1** and **Table 1)** implies 0.5μM iron-binding equivalents (IBE) at 1μM ELT. Comparison of iron mobilisation by 1μM ELT with DFP, DFO and DFX in HuH7 or H962 cardiomyocytes is shown in **Table 2** (top 4 rows)**.** In HuH7, ELT was less effective than DFP, DFX, and DFO at 1μM. In contrast to the lower efficacy of ELT than other chelators in HuH7 cells, 1μM ELT mobilised more iron than DFO, DFX or DFP in H9C2 cells (**Table 2**). The relevance of ELT metabolism to its relative efficacy in HuH7 and H962 is discussed below.

As cell viability could influence iron release independently of chelation, experiments were only performed where baseline viability exceeded 98%, as assessed by the LDH assay. Hepatocytes showed no signs of toxicity following 8 hours of ELT treatment up to 30μM. By contrast, cardiomyocyte viability after 8 hours of exposure to 30μM ELT fell to 93%. Thus some iron release in cardiomyocytes at 30μM (**Figure 2B**) could be partially attributed to toxicity.

ELT decreases cellular ferritin

We next wished to determine how changes in total cellular iron were paralleled by changes in cellular ferritin. When cells were iron-loaded (see methods), tissue ferritin increased by 75% in HuH7 and by 33% in H9C2. After treatment with 10μM ELT for 8 hours, 85% ferritin reduction was seen in HuH7 and 46% in H9C2 cells (**Figure 2C, D**). Respective decrements in cellular iron were 25% in HuH7 and 65% in H9C2 cells. Thus ELT decreased total cellular iron and cellular ferritin in both cell types, with ferritin decrements being proportionately greater in HuH7 than H9C2 cells. Thus ferritin in HuH7 cells appears more responsive, both to iron-loading and unloading than in H9C2 cells, consistent with the known higher iron-storage capacity of hepatocytes.

ELT decreases ROS more rapidly than other chelators

Intracellular ROS generation by iron is predominantly determined by the LIP concentration[31]. Unlike measurement of total cellular iron or ferritin, continuous real-time measurement of ROS is achievable, allowing insight into kinetics of chelation. In **Figure 3A, B** the ROS generation rate is rapidly decreased by ELT in HuH7 and H9C2 cells, even at the first measurable time-points. Inhibition of ROS by DFO was relatively slow, consistent with the known slow cellular uptake of DFO[14], while DFP and DFX have intermediate effects. In **Figure 3C, D,** the inhibitory effects of 10μM ELT and other chelators at 10μM IBE (except CP40 at 33μM IBE) are shown in HuH7, H9C2 and RINm5F cells. ROS generation is inhibited with ELT by 73% in HuH7 and by 61% in H9C2 cells, more than with other chelators at comparable concentrations. In **Table 3 (**top 4 rows) ROS inhibition at 1μM is shown, where ELT has the greatest effect. Thus rapid ROS decrements are similar both in hepatocytes and cardiomyocytes, unlike iron mobilisation. The slower mobilisation of total cellular iron will allow time for metabolic inactivation of ELT in hepatocytes, hence decrease activity of ELT in these cells.

Eltrombopag decreases cellular iron and reverses iron-mediated suppression of insulin secretion in the pancreatic β-cell line (RINm5F)

After RINm5F cells were iron-loaded, 10μM ELT subsequently mobilised a similar amount of iron to 10μM IBE DFO or DFX at 8 hours (**Figure 2E**). ROS inhibition by ELT was found to be dose- sensitive, being greater at 10μM ELT than 3μM ELT (**Figure 3E**). When iron-loading was increased by increasing FBS from 10 to 25%, insulin secretion decreased (**Figure 3F**). Decrements in ROS and cellular iron were associated with restoration of insulin secretion (**Figure 3G**). This was also achieved with DFX but not with DFO or DFP. Restoration of cell function is presumably related to decreasing ROS, secondary to lowering LIP.

Effects of chelator combinations with ELT on iron mobilisation or ROS inhibition

Combinations of chelators may decrease the doses of individual chelators required for a given effect. When DFO, DFP, or DFX at 1μM IBE were combined with 1μM ELT, iron mobilisation was greater than monotherapy with either ELT or a second chelator (**Table 2,** lower 3 rows). The most effective combination was ELT plus DFX, being greater than additive. However ROS inhibition by ELT when combined with other chelators was never more than additive (**Table 3,** lower 3 rows). Iron mobilisation using the combination of ELT (3μM) with the extracellular chelator hydroxypyridinone chelator CP40 (3μM), was also greater than additive (**Figure 2F**), suggesting that entry of a second chelator into cells is not a prerequisite for synergistic chelation (*see discussion and* ***Figure 5C***).

Mechanisms of synergistic iron removal by ELT when combined with DFX or CP40

In a cell-free system, ELT removed iron from pre-formed iron-citrate complexes (**Figure 4A**) faster than DFX (**Figure 4B**) suggesting that ELT accesses some chelateable iron pools faster than DFX. Preformed complexes of ELT also donated iron to DFX (**Figure 4C**) or CP40 (**Figure 4D**) more rapidly than preformed ferric citrate complexes donated iron to DFX. Donation to DFX was most rapid at ELT:iron ratios of 2:1 or 3:1 (**Figure 4E**). Thus ELT appears to satisfy the requirements of an iron-shuttle [36], capable of both rapid iron chelation

as well as iron donation to a second chelator. As DFX is known to enter cells and chelate iron directly[32], DFX could in principle act as a sink for chelated iron within the cells, which is unlikely with CP40.

Greater than additive chelation with DFX or CP40 could in principle also occur by inhibiting re-uptake of iron from ELT complexes. In **Figure 5A**, ELT iron complexes donated iron to HuH7 cells. This was inhibited by the extracellular chelator CP40 but not by DFX (**Figure 5A**). However, DFX complexes can also donate iron to cells (**Figure 5B**) whereas CP40 does not[33]. This we attribute to the lipophilicity of DFX-iron complex, but the marked hydrophilicity of the CP40-iron complex [11,12]. **Figure 5C** suggests a mechanistic scheme for cellular iron mobilisation by ELT alone, or combined with CP40. This involves cellular uptake of ELT and chelation of LIP, which we have not measured directly but which is consistent with several lines of direct and indirect evidence (see discussion).

DISCUSSION

We have demonstrated progressive removal of total cellular iron by ELT in H9C2, HuH7 and RINm5F cell lines. This is associated with lowering of intracellular ferritin, consistent with decrements in storage iron (although storage iron was not measured directly). This was also associated with decrements in ROS and, with restoration of insulin secretion in iron-loaded RINm5F cells. In H9C2 cardiomyocyte derived cells, ELT proved superior at mobilizing cellular iron to licensed iron chelators (DFO, DFP, and DFX), at a relatively low concentration. In, the human hepatocellular HuH7 line, 1μM ELT was less effective than in the rat cardiomyocyte H9C2 cell line (**Table 2**) but was increasingly effective at higher concentrations (**Figure 2A**). Rapid metabolism of ELT in HuH7 cells may decrease efficacy. ELT is metabolized by mono-oxygenation and glucuronidation, with liver conjugation preceding elimination in faeces and urine [34]. Hepatocytes are typically more active in drug metabolism than cardiomyocytes, and HuH7 cells contain most of the Phase I and Phase II enzymes present in hepatocytes[35]. Thus greater metabolic inactivation of ELT would be expected in HuH7 than H9C2 cells. Indeed CYP2B1, 2B2, 2E1 and 2J3 are expressed at lower levels in H9C2 and myocardium than in hepatocytes[36]. As H9C2 cells are rat- rather than human-derived, inter-species differences in metabolism could contribute to the observed differences. In clinical use however, metabolic inactivation of ELT is unlikely to be a major issue limiting iron chelation, as un-metabolized ELT accounts for >94% of drug at 4h with 64% remaining un-metabolized at 24h[34]. The low ELT concentrations that is effective in cell culture may not necessarily translate to animal and clinical studies, particularly if metabolism, distribution, and elimination of iron complexes differ significantly in vivo. The effectiveness and doses of ELT required in vivo, alone or in combination with a second chelator, therefore need to be established.

While we have not measured ELT entry into cells directly, we believe based on several independent lines of evidence that rapid cellular uptake of ELT is likely. Firstly, ELT is taken up rapidly into isolated hepatocytes[37] and neuronal cells[38]. Secondly, studies with other chelators, have shown that chelator entry into cells is key to cellular iron mobilisation. The high lipophilicity and low molecular weight of ELT (**Table 1**) are properties associated with cellular uptake and high chelator efficacy [11-14]. Thirdly, rapid ROS inhibition by ELT supports rapid cellular uptake. ROS inhibition appears to involve *direct* interaction of ELT with ROS[4], which would require intracellular uptake by ELT. Fourthly, ELT rapidly lowers

labile intracellular iron[3], the kinetics of which are more consistent with rapid ELT entry into cells than with secondary effects of iron depletion. Fifthly, the lower cellular iron mobilisation by ELT in HuH7 than H9C2 cells (contrasting with similar decrements in ROS) is consistent with greater metabolic inactivation in HuH7 cells, which itself requires intracellular access by ELT.

Our data show greater-than-additive cellular iron mobilisation by combinations of ELT with either DFX or CP40, whereas additive effects are seen with DFO and DFP. Consideration of iron-binding constants (pFe) and speciation plots for these chelators (**Table 1**) suggested that iron shuttling by ELT might account for the enhanced effects when combined with DFX or CP40. The phenomenon of iron shuttling has been described with other chelator combinations[11, 39-41], where one chelator possessing rapid access to iron pools subsequently donates iron to a 'sink' chelator possessing greater stability for iron(III) binding but slower kinetic access. In principle a second chelator could act as a sink for iron chelated by ELT either within or outside cells. While the low molecular weight and lipophilicity of ELT, both as a free ligand and as iron complexes, are well suited to iron shuttling across cell membranes[42], it is not essential for the 'sink' chelator to enter cells for synergism to occur [42]. The donation of iron from ELT complexes to CP40 extracellularly could explain why CP40, which has no inherent iron-mobilising effects of its own due to its inability to enter cells, enhances iron chelation when combined with ELT. Indeed this mechanism has been described with other iron chelators in combination with CP40[42]. While the speciation plots in **Figure 1B, C, D, E** predict that iron will eventually be donated by ELT onto DFX or DFO, they provide no direct evidence for the rate at which this occurs. We therefore undertook additional experiments in cell-free systems. ELT accessed citrate-bound iron faster than DFX (**Figure 4A, B**), which would accelerate net iron chelation, particularly if the iron was then donated to DFX as a shuttling effect. Indeed, we found iron donation from ELT complexes to DFX or CP40 at rates sufficient to account for enhanced chelation (**Figure 4C. D**). However, we also found that re-uptake of iron from chelate-iron complexes needs to be accounted for. CP40 inhibited iron uptake from ELT complexes (**Figure 5A**) whereas DFX did not (**Figure 5B**). This may relate to DFX-iron complexes themselves being taken into cells (**Figure 5B**), unlike those of CP40. Based on these observations, and the speciation plot data, we have suggested an overall scheme for how greater-than-additive cellular iron removal may occur both extracellularly and intracellularly (**Figure 5C**). In this scheme, the greater-than-additive iron mobilisation seen when CP40 was combined with ELT is mainly

achieved extracellularly by CP40 (shown as L) accepting iron chelated by ELT, allowing ELT to become available for further iron chelation. The iron from the CP40-iron complex is not taken back up into cells whereas iron can be donated by DFX complexes to cells (**Figure 5B**), most of the greater-than-additive iron mobilisation obtained by combining DFX (not shown) with ELT occurs intracellularly, through accelerated chelation of LIP by ELT compared with DFX.

Our data are consistent with the iron-chelating effects of ELT being independent of the TPO-R effect because the latter is highly species-specific[3, 43]. The thrombopoietic actions of ELT occur only in humans and primates with no effect in rodents, whereas the iron mobilizing effects in our experiments were seen both in human HuH7 cells and rat H9C2 cardiomyocyte and RINm5f pancreatic cells. The chelating actions of ELT could be clinically beneficial in several settings. An obvious application would be the treatment of transfusional iron overload. The elimination route for iron complexes of ELT is currently unknown and requires studies in animal models and in humans. Inter-species differences in metabolism and routes of elimination of iron complexes are well established with other chelators and may be unpredictable from first principles[22]. However, if iron chelated by ELT is donated to a second chelator such as DFX, then the ELT iron complex would not need to be eliminated in urine or faeces directly. This will need to be demonstrated in vivo however.

In addition to increasing platelet counts, ELT can increase red cell and neutrophil counts and is approved in the US for the treatment of severe aplastic anemia[44]. Some effects of ELT on hematopoiesis in MDS and aplastic anemia might be derived from this iron-chelating mechanism. As our data suggest that ELT-iron complexes can also donate iron to cells, iron redistribution should also be examined as a mechanism for improved haematopoiesis. Anti-leukemic effects mediated through modulation of intracellular iron content have also been postulated[3]. The antioxidant and iron-chelation properties are tightly linked to cell death in leukemia cells[3] as the anti-proliferative and apoptotic effects of chelators are well described[17, 45], through mechanisms that include ribonucleotide reductase inhibition[16]. However, in patients with ITP, iron chelation could create or exacerbate iron deficiency, which needs to be explored. Importantly, the 1μM ELT concentration that mobilised cellular iron is nearly twenty-fold less than peak plasma concentrations obtained following 30mg ELT orally[30]. At this dose, platelet increments do not typically exceed 1.2 x baseline in healthy volunteers with repeat dosing[46]. Hence, in principle, effective chelating doses could be given without

promoting unacceptable thrombocytosis, although requiring careful clinical study. In principle, still lower concentrations could be used when combined with a clinically licensed chelator. ELT has been generally well-tolerated long-term[47], the most common adverse events being: headache, gastrointestinal symptoms, and upper respiratory tract infections[47]. Published studies did not demonstrate any correlation between ELT treatment and occurrence of thromboembolic events[48-51]. This suggests that ELT doses that induced significant intracellular chelation could be administered to non-thrombocytopenic patients without appreciable changes in platelet counts.

In conclusion, we have demonstrated for the first time the iron-binding properties of ELT and its iron-mobilizing properties from cells in culture. Decrements in ROS and improved cell function were also observed. Single agent ELT mobilised intracellular iron at concentrations similar to or lower than clinically licensed chelators, particularly from H9C2 cells. Additive or synergistic intracellular chelation with clinically available chelators has been shown. It will be important to demonstrate whether these *in vitro* effects and effective doses translate to iron-overloaded animals and ultimately to the clinical setting.

Acknowledgements

We would like to thank the Onassis Foundation, Athens, Greece for their support in the form of a PhD Scholarship. Prof Porter is supported by the Bio- medical Research Centre, UCL. J.P. and N.C have received honorarium for consultancy work and speaking at educational events sponsored by Novartis

Authorship

Contribution: E.V., Y.C., M.G., B.P., N.C., M.G., B.H., J.P., designed research, E.V., Y.C. M.G. and P.S. performed research, E.V., Y.C., B.H., M.G. and J.P. analysed and interpreted data, E.V., Y.C., B.H. and J.P. wrote the manuscript.

Conflict of interest disclosure: The authors declare no competing financial interests.

FIGURE LEGENDS

Figure 1. Structure and iron-binding properties of ELT. Data on the iron-binding properties of ELT were obtained specifically for this paper and are not previously published elsewhere. The iron-binding properties of other chelators are based on previously published data[11, 19]. (**a**) Structure of ELT and its iron complexes are shown. The free ligand possesses 2 tautomers (**1** and **2**). Three major iron(III) complexes have been identified: **3** (FeELT), **4** ($FeELT_2H$) and **5** ($FeELT_2$). (**b**) The speciation of iron(III) in the presence of ELT as a function of pH. $[Fe]_{total}$=1μM; $[ELT]_{total}$=10μM is shown at steady state (i.e. when sufficient time has elapsed for the reactions to go to completion). These proportions are calculated from the iron-binding constants for iron-chelate complexes of the respective chelators shown in **Table 1** and determined as described in methods**.** Titration with iron(III) yielded three equilibrium constants: K_{FeL}=25.6, K_{FeL_2H}=43.4, and K_{FeL_2}= 34.9. ELT has three pK_a values (the pH at which half the molecules are ionised) of 2.6, 8.7, 11.1. Using these data, a pFe value of 22.0 (the strength of iron(III) binding, being the negative log of the unbound iron(III) concentration under defined conditions (1μM iron(III) and 10μM chelator[52]) was determined, which is greater than that of DFP (20.4) and very similar to that of DFX (23.1). Competition between ELT and other chelators for iron(III) are shown for (**c**) 1μM DFO, (**d**) 3μM DFP (**e**) 2μM DFX. These show the predicted proportions of each ELT iron complex when mixed with a second chelator, after reactions have gone to completion (in steady state). Thus for example, at 1μM ELT over 99% of iron(III) will be bound to DFO (**c**), whereas under the same conditions about half of the iron will be bound to DFP (**d**) and about 70% to DFX (**e**).

Figure 2. Cellular iron mobilisation and/or ferritin iron decrements with ELT from HuH7, H9C2 and RINm5F cells. (**a**) Dose response for iron release from HuH7 cells at 8h is shown. (**b**) Dose response for iron release from H9C2 cells at 1, 2, 4 and 8 hours is shown. Cells were loaded with iron as described in methods. Adherent cells were rinsed four times, including one wash containing DFO at 30μM IBE and 3 PBS washes, and subsequently exposed to ELT and other chelators for the times shown. Chelator-containing supernatants were then removed, and the cells washed four times as above before lysing with 200mM NaOH. Intracellular iron concentration was then determined at each time point using the ferrozine assay described in methods and normalised for total cellular protein in each well. Results shown are expressed as the % of T_0 cellular iron released at the times shown and are the mean±SEM of 6 replicates in one representative experiment. (**c**) Iron release by ELT

10μM and DFO, DFP and DFX 10μM IBE following 8 hours of treatment in RINm5F cells. Cells were iron-loaded using two 10-hour changes of 10% FBS-containing RPMI media and rinsed as above. Comparison of the effect of ELT on ferritin and total cellular iron mobilisation in (**d**) HuH7 hepatocyte and (**e**) H9C2 cardiomyocyte cells is shown. Following iron loading, chelator treatment for 8 hours and rinsing, iron content was ascertained as described above. Ferritin was quantified using commercially available ELISA kits appropriate for our rat and human cell lines. Results are expressed as the % of T_0 cellular iron mobilised or decrement of ferritin expressed as % of T_0 values at the times shown and are the mean±SEM of 3 replicates of one representative experiment.

Figure 3. Effect of ELT and iron chelators on intracellular ROS generation and cell function (insulin production) in iron-loaded cells. The time-course for ROS inhibition by ELT and other chelators are shown in **(a)** HuH7 or **(b)** H9C2 cells. Cells were iron-loaded and then rinsed four times as described above. Chelators were then added, and the rate of change of ROS production was recorded as fluorescence change (excitation at 504 nm, emission at 526 nm) continuously over 1 hour in the plate reader at 37^{o}C. DFO, DFP, and DFX were used at 10μM IBE, and ELT at 10μM. The rate of ROS production was compared between chelator-treated and chelator-untreated cells. Data shown are readings from individual plates. ROS rate inhibition at 1h with CP40, DFO, DFP, DFX, and ELT are shown in (**c**) HuH7 and (**d**) H9C2 cells at 10μM IBE for each chelator and 10μM ELT and 33μM IBE CP40. 10μM ELT shows greater inhibition of ROS in both cell types than other chelators at the same concentration in both HuH7 and H9C2 cells. The extracellular hydroxypyridinone chelator, CP40, had no effect on ROS. (**e**) Effect of chelator treatment over a 90-minute period in RINm5F cells on ROS generation is shown. Results are the mean±SEM of 4 observations in one experiment. (**f**) Effect of iron loading in RINm5F cells with two changes of RPMI media containing 10-25% FBS on insulin secretion. Following treatment, cells were challenged with Kreb's Ringer Buffer containing glucose and insulin concentration in the supernatant determined as described in methods. (**g**) Effect of chelation treatment on insulin production in RINm5F cells iron-loaded with two 10-hour changes of RPMI media containing 25% FBS. (* $p<0.05$, ** $p<0.01$ compared to control). Results are the mean ± SEM of 3 observations in one experiment.

Figure 4. Rates of iron chelation and exchange between ELT and DFX in vitro

The rates of ferric-chelate complex formation from preformed ferric-citrate complexes (iron:

citrate 10:100μM) are shown with either (**a**) ELT (30μM), (monitored at 614nm which form a secondary peak of ELT-Fe complex), or (**b**) DFX (30μM) (monitored at 556nm, secondary peak for DFX-iron complex). The top horizontal line represents 100% iron complex formation of ELT or DFX (10μM iron(III)). The lower horizontal lines represent the absorbances of the iron-free ligands (30μM). It can be seen that ELT binds iron from ferric citrate complexes faster than DFX. The 50% effect is achieved at about 180 min for ELT, but later at around 300 min for DFX. The 100% effect is achieved by ELT at about 12 hours whereas DFX takes approximately 33 hours. (**c**) The rates of ferric-DFX complex formation (300μM of DFX) from either preformed ferric-citrate (iron:citrate 10:100μM) or from ferric-ELT (10μM, 1:2) is shown. It can be seen that DFX binds iron from preformed complexes of ELT faster than from ferric-citrate complexes (**d**) Rate of CP40 ferric complex formation is shown (at 200μM IBE CP40 from preformed 10μM $FeELT_2$. The reaction is completed at approximately 200 minutes. (**e**) The effect of excess ELT ratio to iron on the rate of DFX chelation from preformed iron(III):ELT complexes (ratios 1:1 , 1:2, 1:3 and 1:10) and 3.33, 6.66, 10, 33.3μM ELT, respectively) are shown. Iron complexes of DFX form more rapidly and most completely when the ratio is 1:2 and 1:3 than with ratios of 1:1. A 10-fold excess of iron-free ELT to iron retards the rate of iron donation to DFX.

Figure 5. Cellular uptake of iron complexes of ELT, interactions with DFX and CP40 and proposed mechanisms of interaction of ELT with chelatable cellular iron and effects of second chelator. Iron uptake into HuH7 cells from preformed chelate complexes of ELT or DFX is shown at 6h, in panels (**a**) and (**b**) of the same experiment. Control iron release with ELT or CP40 (**a**) or DFX alone (**b**) are also shown. CP40 was chosen for evaluation because of its lack of iron removal from cells when used as a single agent and its lack of iron donation to cells. After incubation, cells were washed, the first wash containing DFO at 30μM IBE and then with 3 PBS washes before intracellular iron concentration was determined using the ferrozine assay as described in the methods. (**a**) Iron uptake from chelate complexes of ELT is shown, where complexes of ELT were presented either as 1:1 or 1:2 ratios of iron:ELT. CP40 inhibits iron uptake from both FeELT and FeELT2. (**b**) In contrast to CP40, DXF does not inhibit the net uptake of iron from preformed complexes of ELT. Preformed complexes of DFX (DFX2Fe) donate some iron to cells but less than from complexes of ELT. **(c)** Proposed mechanisms of interaction of ELT with cellular iron with or without a second chelator. ELT diffuses into cells, rapidly binding LIP iron thus decreasing ROS. Iron complexes of ELT then diffuse out of the cell, some of which can subsequently

donate iron back to the cell (**Figure 5A**). Diffusion of ELT into cells was not measured directly but has been previously shown in other cells and is consistent with its low molecular weight, its high lipid solubility and rapid intracellular ROS inhibition. A second chelator (L) can increase intracellular iron chelation and thus cellular iron release if it gains direct access to LIP, as is known to occur with DFX but not with CP40. ELT binds chelateable iron (from citrate) faster than DFX (**Figure 4A** and **B**). DFX binds iron from complexes of ELT faster than those bound to citrate (Fe:citrate 10:100) (**Figure 4C**). A second chelator can also increase net iron release extracellularly by competitive removal of iron from ELT-iron complexes, thus decreasing the donation of iron from ELT-iron complexes to cells. Both intracellular and extracellular donation of iron to a second chelator (L) potentially frees up ELT for a further round of iron chelation.

TABLES

Table 1. Comparison of the structure and iron-binding properties of ELT and other chelators. Binding properties of ELT are not previously described and were determined specifically for for this paper. The relative stabilities of iron(III) binding are represented by the pFe, where the pFe of a given chelator for iron(III) is the negative log of the uncoordinated metal concentration under defined conditions[53]. The higher the pFe values, the lower the concentration of uncoordinated iron(III) and hence the greater stability for the iron-chelate complex. ELT can form neutrally charged 1:1 complexes with iron(III) or 3- negatively charged 2:1 complexes. Properties of other chelators use published data[11,19], except for the pFe value of DFX where 23.1 is used based on the properties of the molecule in 100% water; The widely adopted values of 22.4 or 22.5, are based on titrations run in 20% DMSO. When pairs of chelators are combined in solution, iron(III) will bind preferentially to the chelator with the higher pFe value. This is highest for DFO and lowest for DFP, with DFX having an intermediate value but greater than ELT. DFO, desferrioxamine; DFP, deferiprone; DFX, deferasirox; Kpart, partition coefficient[54-56].

Table 2. Comparison of percentage of intracellular iron mobilised at 8hours in a cardiomyocyte (H9C2) and a hepatocyte (HuH7) cell lines by clinically available chelators or ELT, alone (top panel) or in combination (lower panel). Chelator concentrations are expressed as iron-binding equivalents (IBE). Cells were pre-loaded with iron, rinsed, incubated with chelators, and cellular iron determined as described in **Figure 2**. Results shown as the % iron released expressed as a % of T_0 cellular iron and are the mean±SEM of 4 replicates in one experiment.

Table 3. Comparison of ROS generation in cardiomyocyte (H9C2) and a hepatocyte (HuH7) cell lines is shown after addition of clinically available chelators or ELT, alone (top panel) or in combination (lower panel) over 90 minutes. Experimental design and determination of ROS is otherwise as described in **Figure 3**. Results are the mean±SEM of 4 observations in one experiment. (* $p<0.05$, ** $p<0.01$ compared to control).

REFERENCES

1. Williams DD, Peng B, Bailey CK, Wire MB, Deng Y, Park JW, et al. Effects of food and antacids on the pharmacokinetics of eltrombopag in healthy adult subjects: two single-dose, open-label, randomized-sequence, crossover studies. Clinical therapeutics. 2009;31:764-76.
2. Wire MB, Bruce J, Gauvin J, Pendry CJ, McGuire S, Qian Y, et al. A randomized, open-label, 5-period, balanced crossover study to evaluate the relative bioavailability of eltrombopag powder for oral suspension (PfOS) and tablet formulations and the effect of a high-calcium meal on eltrombopag pharmacokinetics when administered with or 2 hours before or after PfOS. Clinical therapeutics. 2012;34:699-709.
3. Roth M, Will B, Simkin G, Narayanagari S, Barreyro L, Bartholdy B, et al. Eltrombopag inhibits the proliferation of leukemia cells via reduction of intracellular iron and induction of differentiation. Blood. United States2012. p. 386-94.
4. Kalota A, Selak MA, Garcia-Cid LA, Carroll M. Eltrombopag modulates reactive oxygen species and decreases acute myeloid leukemia cell survival. PloS one. 2015;10:e0126691.
5. Kurokawa T, Murata S, Zheng YW, Iwasaki K, Kohno K, Fukunaga K, et al. The Eltrombopag antitumor effect on hepatocellular carcinoma. International journal of oncology. 2015;47:1696-702.
6. Svensson T, Chowdhury O, Garelius H, Lorenz F, Saft L, Jacobsen SE, et al. A pilot phase I dose finding safety study of the thrombopoietin-receptor agonist, eltrombopag, in patients with myelodysplastic syndrome treated with azacitidine. European journal of haematology. 2014;93:439-45.
7. Leitch HA, Vickars LM. Supportive care and chelation therapy in MDS: are we saving lives or just lowering iron? Hematology Am Soc Hematol Educ Program. United States2009. p. 664-72.
8. Olnes MJ, Scheinberg P, Calvo KR, Desmond R, Tang Y, Dumitriu B, et al. Eltrombopag and improved hematopoiesis in refractory aplastic anemia. The New England journal of medicine. 2012;367:11-9.
9. Vlachodimitropoulou E, Cooper N, Psaila B, Sola-Visner M, Porter J. Eltrombopag Mobilizes Intracellular Iron Stores at Concentrations Lower Than Those Required with Other Clinically Available Iron Chelators. Blood. 2014;124.
10. Vlachodimitropoulou E, JB P, Cooper N, Psaila B, Sola-Visner M. A Potential Novel Application of Eltrombopag: A Combination Agent to Enhance Iron Chelation Therapy. Blood. 2015;126:353.
11. Vlachodimitropoulou Koumoutsea E, Garbowski M, Porter J. Synergistic intracellular iron chelation combinations: mechanisms and conditions for optimizing iron mobilization. British journal of haematology. 2015;170:874-83.
12. Porter JB, Gyparaki M, Burke LC, Huehns ER, Sarpong P, Saez V, et al. Iron mobilization from hepatocyte monolayer cultures by chelators: the importance of membrane permeability and the iron-binding constant. Blood. 1988;72:1497-503.
13. Porter JB, Morgan J, Hoyes KP, Burke LC, Huehns ER, Hider RC. Relative oral efficacy and acute toxicity of hydroxypyridin-4-one iron chelators in mice. Blood. 1990;76:2389-96.
14. Hoyes KP, Porter JB. Subcellular distribution of desferrioxamine and hydroxypyridin-4-one chelators in K562 cells affects chelation of intracellular iron pools. British journal of haematology. 1993;85:393-400.
15. Cooper CE, Lynagh GR, Hoyes KP, Hider RC, Cammack R, Porter JB. The relationship of intracellular iron chelation to the inhibition and regeneration of human ribonucleotide reductase. The Journal of biological chemistry. 1996;271:20291-9.

16. Kayyali R, Porter JB, Liu ZD, Davies NA, Nugent J, Cooper CE, et al. Structure-function investigation of the interaction of 1- and 2- substituted 3-hydroxypyridin-4-ones with 5-lipoxygenase and ribonucleotide reductase. The Journal of biological chemistry. 2001;15:15.
17. Hoyes KP, Hider RC, Porter JB. Cell cycle synchronization and growth inhibition by 3-hydroxypyridin-4-one iron chelators in leukemia cell lines. Cancer research. 1992;52:4591-9.
18. Maclean KH, Cleveland JL, Porter JB. Cellular zinc content is a major determinant of iron chelator-induced apoptosis of thymocytes. Blood. 2001;98:3831-9.
19. Porter J, Hershko C. The properties of Clinically useful Iron Chelators Iron Phyisology and Pathophysiology in Humans , Editors Anderson HJ and McLaren GD Humana Press (Book) 2012;Chapter 28:591-630.
20. Ma Y, Kong X, Chen Y-l, Hider RC. Synthesis and characterizations of pyridazine-based iron chelators. 2014.
21. Porter JB, Singh S, Hoyes KP, Epemolu O, Abeysinghe RD, Hider RC. Lessons from preclinical and clinical studies with 1,2-diethyl-3- hydroxypyridin-4-one, CP94 and related compounds. Adv Exp Med Biol. 1994;356:361-70.
22. Porter JB, Abeysinghe RD, Hoyes KP, Barra C, Huehns ER, Brooks PN, et al. Contrasting interspecies efficacy and toxicology of 1,2-diethyl-3-hydroxypyridin-4-one, CP94, relates to differing metabolism of the iron chelating site. British journal of haematology. 1993;85:159-68.
23. Gans P, O'Sullivan B. GLEE, a new computer program for glass electrode calibration. Talanta. 2000;51:33-7.
24. Gans P, Sabatini A, Vacca A. Determination of equilibrium constants from spectrophometric data obtained from solutions of known pH: the program pHab. Annali di chimica. 1999;89:45-9.
25. Alderighi L, Gans P, Ienco A, Peters D, Sabatini A, Vacca A. Hyperquad simulation and speciation (HySS): a utility program for the investigation of equilibria involving soluble and partially soluble species. Coordination Chemistry Reviews. 1999;184:311-8.
26. Evans RW, Rafique R, Zarea A, Rapisarda C, Cammack R, Evans PJ, et al. Nature of non-transferrin-bound iron: studies on iron citrate complexes and thalassemic sera. J Biol Inorg Chem. 2008;13:57-74.
27. Lu TH, Su CC, Chen YW, Yang CY, Wu CC, Hung DZ, et al. Arsenic induces pancreatic β-cell apoptosis via the oxidative stress-regulated mitochondria-dependent and endoplasmic reticulum stress-triggered signaling pathways. Toxicol Lett. 2011;201:15-26.
28. Praz GA, Halban PA, Wollheim CB, Blondel B, Strauss AJ, Renold AE. Regulation of immunoreactive-insulin release from a rat cell line (RINm5F). The Biochemical journal. 1983;210:345-52.
29. www.molinspiration.com.
30. Gibiansky E, Zhang J, Williams D, Wang Z, Ouellet D. Population pharmacokinetics of eltrombopag in healthy subjects and patients with chronic idiopathic thrombocytopenic purpura. Journal of clinical pharmacology. 2011;51:842-56.
31. Cabantchik ZI. Labile iron in cells and body fluids: physiology, pathology, and pharmacology. Front Pharmacol. 2014;5:45.
32. Glickstein H, El RB, Link G, Breuer W, Konijn AM, Hershko C, et al. Action of chelators in iron-loaded cardiac cells: Accessibility to intracellular labile iron and functional consequences. Blood. 2006;108:3195-203.
33. Garbowski MW EP, Vlachodimitropoulou E, Hider R, Porter JB. Residual erythropoiesis protects against myocardial hemosiderosis in transfusion-dependent thalassemia by lowering labile plasma iron via transient generation of apotransferrin. Haematologica (Accepted 19th June 2017). 2017.

34. Deng Y, Madatian A, Wire MB, Bowen C, Park JW, Williams D, et al. Metabolism and disposition of eltrombopag, an oral, nonpeptide thrombopoietin receptor agonist, in healthy human subjects. Drug metabolism and disposition: the biological fate of chemicals. 2011;39:1734-46.
35. Guo L, Dial S, Shi L, Branham W, Liu J, Fang JL, et al. Similarities and differences in the expression of drug-metabolizing enzymes between human hepatic cell lines and primary human hepatocytes. Drug metabolism and disposition: the biological fate of chemicals. 2011;39:528-38.
36. Zordoky BN, El-Kadi AO. H9c2 cell line is a valuable in vitro model to study the drug metabolizing enzymes in the heart. Journal of pharmacological and toxicological methods. 2007;56:317-22.
37. Takeuchi K, Sugiura T, Umeda S, Matsubara K, Horikawa M, Nakamichi N, et al. Pharmacokinetics and hepatic uptake of eltrombopag, a novel platelet-increasing agent. Drug metabolism and disposition: the biological fate of chemicals. 2011;39:1088-96.
38. Bastian TW, Duck KA, Michalopoulos GC, Chen MJ, Liu ZJ, Connor JR, et al. Eltrombopag, a thrombopoietin mimetic, crosses the blood-brain barrier and impairs iron-dependent hippocampal neuron dendrite development. J Thromb Haemost. 2017;15:565-74.
39. Srichairatanakool S, Kemp P, Porter JB. Evidence for "shuttle" effect of NTBI onto desferrioxamine in thalassaemic plasma in the presence of NTA. International Symposium: Iron in Biology and Medicine. St. Malo, France1997. p. 210 (abstract).
40. Giardina PJ, Grady RW. Chelation therapy in beta-thalassemia: an optimistic update. Seminars in hematology. 2001;38:360-6.
41. Evans P, Kayyali R, Hider RC, Eccleston J, Porter JB. Mechanisms for the shuttling of plasma non-transferin-bound iron (NTBI) onto deferoxamine by deferiprone. Transl Res. 2010;156:55-67.
42. Vlachodimitropoulou K, E., Garbowski M, Porter J. Synergistic intracellular iron chelation combinations: mechanisms and conditions for optimizing iron mobilization. Br J Haematol. 2015;170:874-83.
43. Erickson-Miller CL, Delorme E, Tian SS, Hopson CB, Landis AJ, Valoret EI, et al. Preclinical activity of eltrombopag (SB-497115), an oral, nonpeptide thrombopoietin receptor agonist. Stem Cells. 2009;27:424-30.
44. Design iW. eltrombopag (Revolade (EU), Promacta (US)) UKMi New Drugs Online Database. 2016.
45. Maclean KH, Cleveland JL, Porter JB. Cellular zinc content is a major determinant of iron chelator-induced apoptosis of thymocytes. Blood. 2001;98:3831-9.
46. Jenkins JM, Williams D, Deng Y, Uhl J, Kitchen V, Collins D, et al. Phase 1 clinical study of eltrombopag, an oral, nonpeptide thrombopoietin receptor agonist. Blood. 2007;109:4739-41.
47. Saleh MN, Bussel JB, Cheng G, Meyer O, Bailey CK, Arning M, et al. Safety and efficacy of eltrombopag for treatment of chronic immune thrombocytopenia: results of the long-term, open-label EXTEND study. Blood. 2013;121:537-45.
48. Bussel JB, Cheng G, Saleh MN, Psaila B, Kovaleva L, Meddeb B, et al. Eltrombopag for the treatment of chronic idiopathic thrombocytopenic purpura. The New England journal of medicine. 2007;357:2237-47.
49. Bussel JB, Provan D, Shamsi T, Cheng G, Psaila B, Kovaleva L, et al. Effect of eltrombopag on platelet counts and bleeding during treatment of chronic idiopathic thrombocytopenic purpura: a randomised, double-blind, placebo-controlled trial. Lancet (London, England). 2009;373:641-8.

50. Bussel JB, Saleh MN, Vasey SY, Mayer B, Arning M, Stone NL. Repeated short-term use of eltrombopag in patients with chronic immune thrombocytopenia (ITP). British journal of haematology. 2013;160:538-46.
51. Cheng G, Saleh MN, Marcher C, Vasey S, Mayer B, Aivado M, et al. Eltrombopag for management of chronic immune thrombocytopenia (RAISE): a 6-month, randomised, phase 3 study. Lancet (London, England). 2011;377:393-402.
52. Vlachodimitropoulou E, JB P, Cooper N, Psaila B, Sola-Visner M. A Potential Novel Application of Eltrombopag: A Combination Agent to Enhance Iron Chelation Therapy. . Blood. 2015;126:353.
53. Martell A. The design and synthesis of chelating agents: Elsevier North Holland Inc; 1981.
54. Ihnat P, Vennerstrom J, Robinson D. Solution equilibria of deferoxamine amides. J Pharm Sci. 2002;91.
55. Motekaitis R, Martell A. Stabilities of the iron(III) chelates of 1,2-dimethyl-3-hydroxy-4-pyridinone and related ligands. Inorganica Chimica Acta. 1991;183:71-80.
56. Nick H, Wong A, Acklin P, Faller B, Jin Y, Lattmann R, et al. ICL670A: preclinical profile. Advances in experimental medicine and biology. 2002;509:185-203.

TABLE 1

	DFO	DFP	DFX	Eltrombopag
Molecular weight	**561**	**139**	**373**	**442**
Chelator / Iron(III) ratio	**1:1**	**3:1**	**2:1**	**2:1 and 1:1**
Log stability constant for iron (III)	**30.6**	**37.2**	**36.5**	**34.9**
pFe (pmol/L)	**26.6**	**20.7**	**23.1**[1]	**22.0**
Charge of free ligand pH 7.4	**1 +**	**0**	**1-**	**1-**
Charge of iron complex at pH7.4	**1+**	**0**	**3^-**	**3^- (2:1); 0 (1:1)**
Lipid solubility free ligand (log P)	**-3**	**-0.8**	**4.3**	**6.3**

[1] Value determined for 100% aqueous system

Table 2

% iron release following 8 hours of chelator treatment

	H9C2 Cardiomyocyte-like cells		HuH7 Hepatocyte-like cells
DFO 1μM ibe	14.2 ± 1.2		28.6 ± 1.4
DFP 1μM ibe	17.1 ± 1.5		25.7 ± 1.2
DFX 1μM ibe	11.7 ± 1.0		22.8 ± 1.7
ELT 1μM	42.1 ± 2.1		6.9 ± 0.3
ELT 1μM + DFO 1μM ibe	58.2 ± 2.5		34.3 ± 1.1
ELT 1μM + DFP 1μM ibe	59.9 ± 3.1		38.2 ± 1.5
ELT 1μM + DFX 1μM ibe	66.4 ± 2.4		51.4 ± 1.9

Table 3

% decrease in ROS generation rate at 90 minutes

	H9C2 Cardiomyocyte–like cells		HuH7 Hepatocyte–like cells
DFO 1µM ibe	12.1 ± 1.3		14.3 ± 0.9
DFP 1µM ibe	29.7 ± 1.3		25.0 ± 1.8
DFX 1µM ibe	33.2 ± 2.7		21.4 ± 2.6
ELT 1µM	42.2 ± 1.7		39.2 ± 2.1
ELT 1µM + DFO 1µM ibe	62.2 ± 3.2		55.1 ± 3.1
ELT 1µM + DFP 1µM ibe	60.3 ± 4.1		60.2 ± 3.2
ELT 1µM + DFX 1µM ibe	57.3 ± 3.3		51.3 ± 2.2

Figure 1

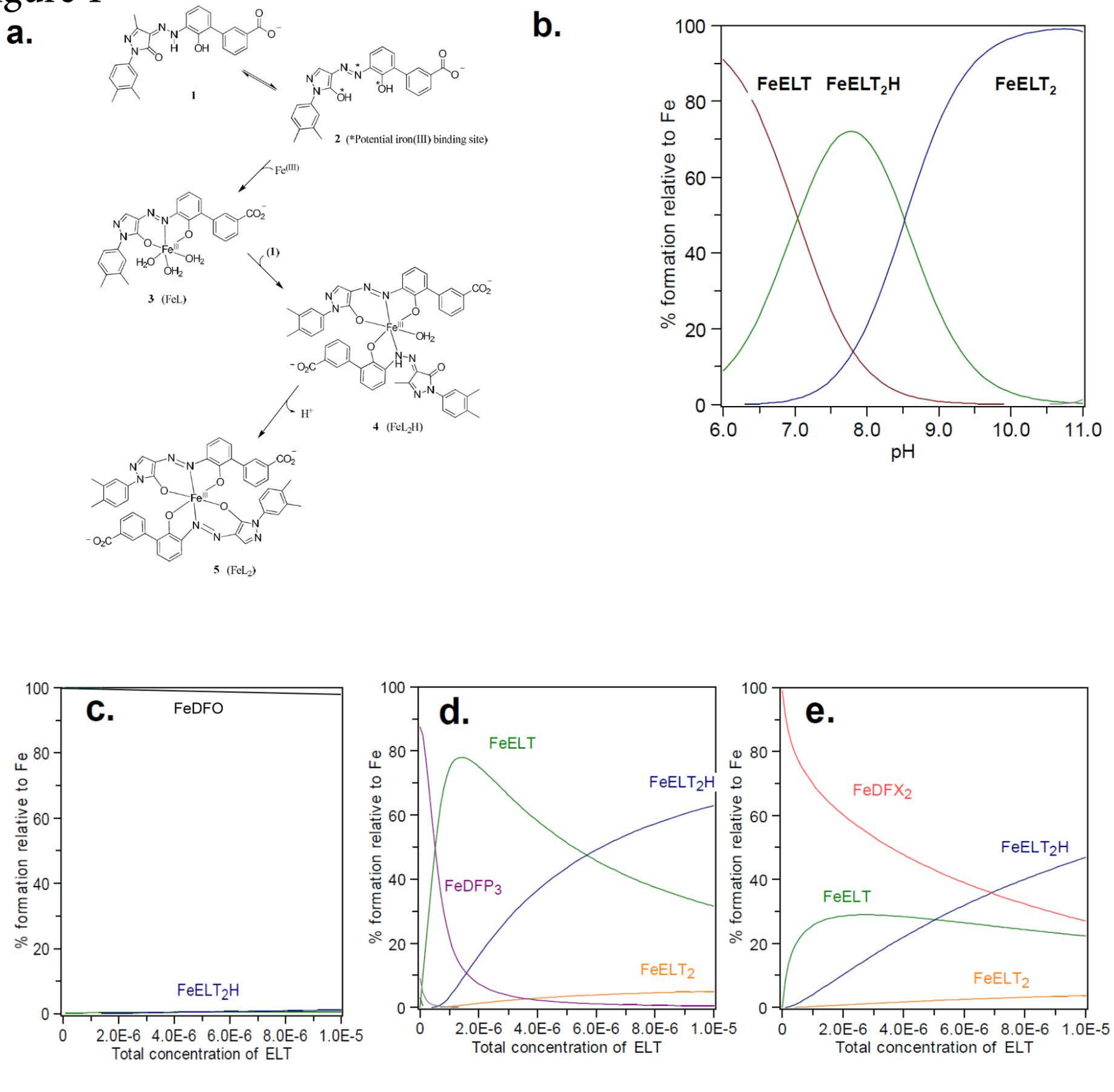
a.
1
2 (*Potential iron(III) binding site)
Fe(III)
3 (FeL)
(1)
4 (FeL2H)
H+
5 (FeL2)
b.
FeELT
FeELT2H
FeELT2
% formation relative to Fe
pH
c.
FeDFO
FeELT2H
d.
FeELT
FeELT2H
FeDFP3
FeELT2
e.
FeDFX2
FeELT2H
FeELT
FeELT2
Total concentration of ELT

Figure 2

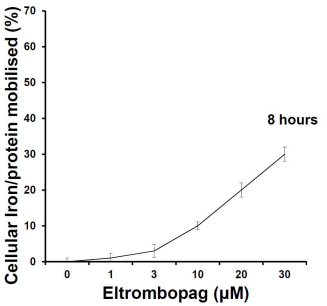
a. HuH7
Cellular Iron/protein mobilised (%)
8 hours
Eltrombopag (μM)

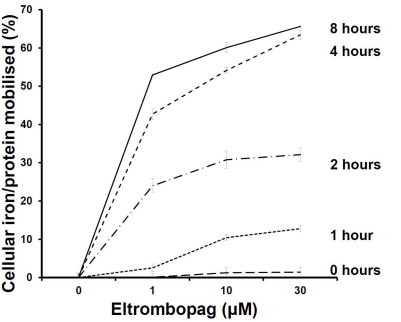
b. H9C2
Cellular iron/protein mobilised (%)
8 hours
4 hours
2 hours
1 hour
0 hours
Eltrombopag (μM)

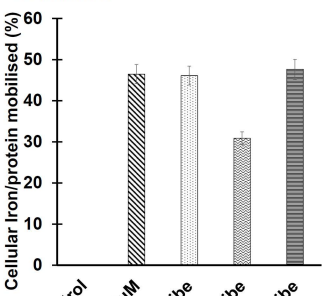
c. RINm5F
Cellular Iron/protein mobilised (%)
Control
ELT 10μM
DFO 10μM ibe
DFP 10μM ibe
DFX 10μM ibe

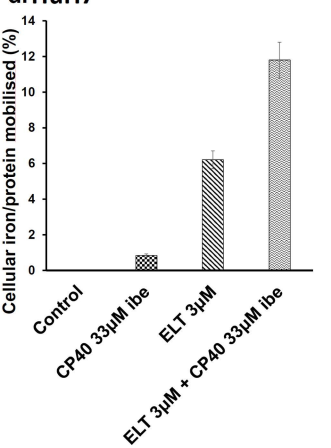
d. HuH7
Cellular iron/protein mobilised (%)
Control
CP40 33μM ibe
ELT 3μM
ELT 3μM + CP40 33μM ibe

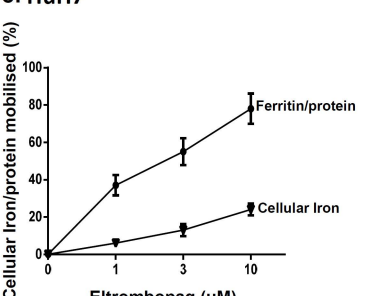
e. HuH7
Cellular Iron/protein mobilised (%)
Ferritin/protein
Cellular Iron
Eltrombopag (μM)

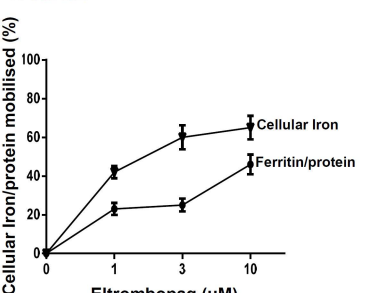
f. H9C2
Cellular Iron/protein mobilised (%)
Cellular Iron
Ferritin/protein
Eltrombopag (μM)

Figure 3

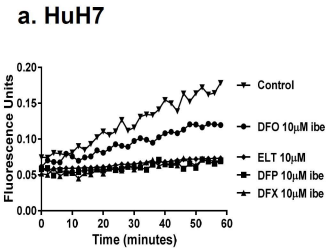
a. HuH7
Fluorescence Units
Time (minutes)
Control
DFO 10μM ibe
ELT 10μM
DFP 10μM ibe
DFX 10μM ibe

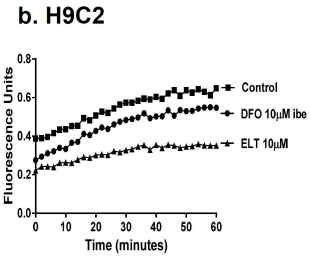
b. H9C2
Fluorescence Units
Time (minutes)
Control
DFO 10μM ibe
ELT 10μM

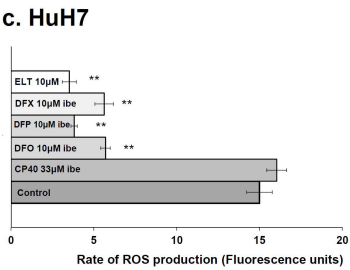
c. HuH7
ELT 10μM
DFX 10μM ibe
DFP 10μM ibe
DFO 10μM ibe
CP40 33μM ibe
Control
Rate of ROS production (Fluorescence units)

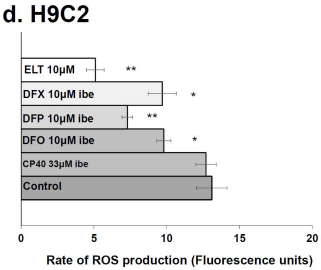
d. H9C2
ELT 10μM
DFX 10μM ibe
DFP 10μM ibe
DFO 10μM ibe
CP40 33μM ibe
Control
Rate of ROS production (Fluorescence units)

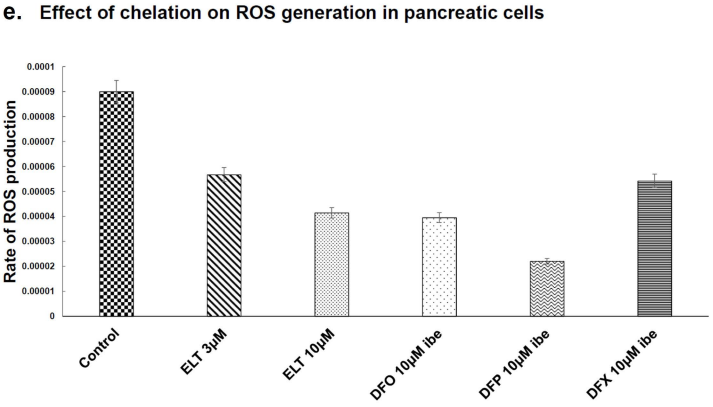
e. Effect of chelation on ROS generation in pancreatic cells
Rate of ROS production
Control
ELT 3μM
ELT 10μM
DFO 10μM ibe
DFP 10μM ibe
DFX 10μM ibe

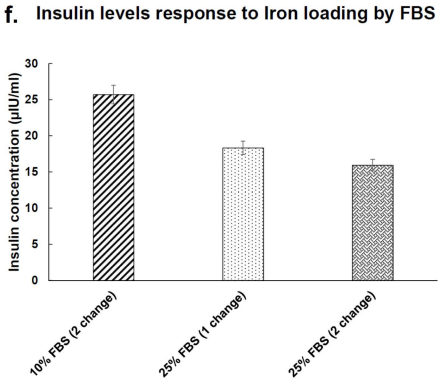
f. Insulin levels response to Iron loading by FBS
Insulin concentration (μIU/ml)
10% FBS (2 change)
25% FBS (1 change)
25% FBS (2 change)

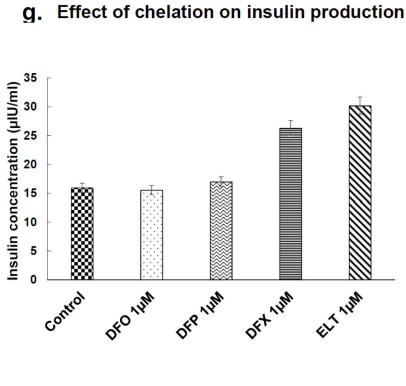
g. Effect of chelation on insulin production
Insulin concentration (μIU/ml)
Control
DFO 1μM
DFP 1μM
DFX 1μM
ELT 1μM

Figure 4

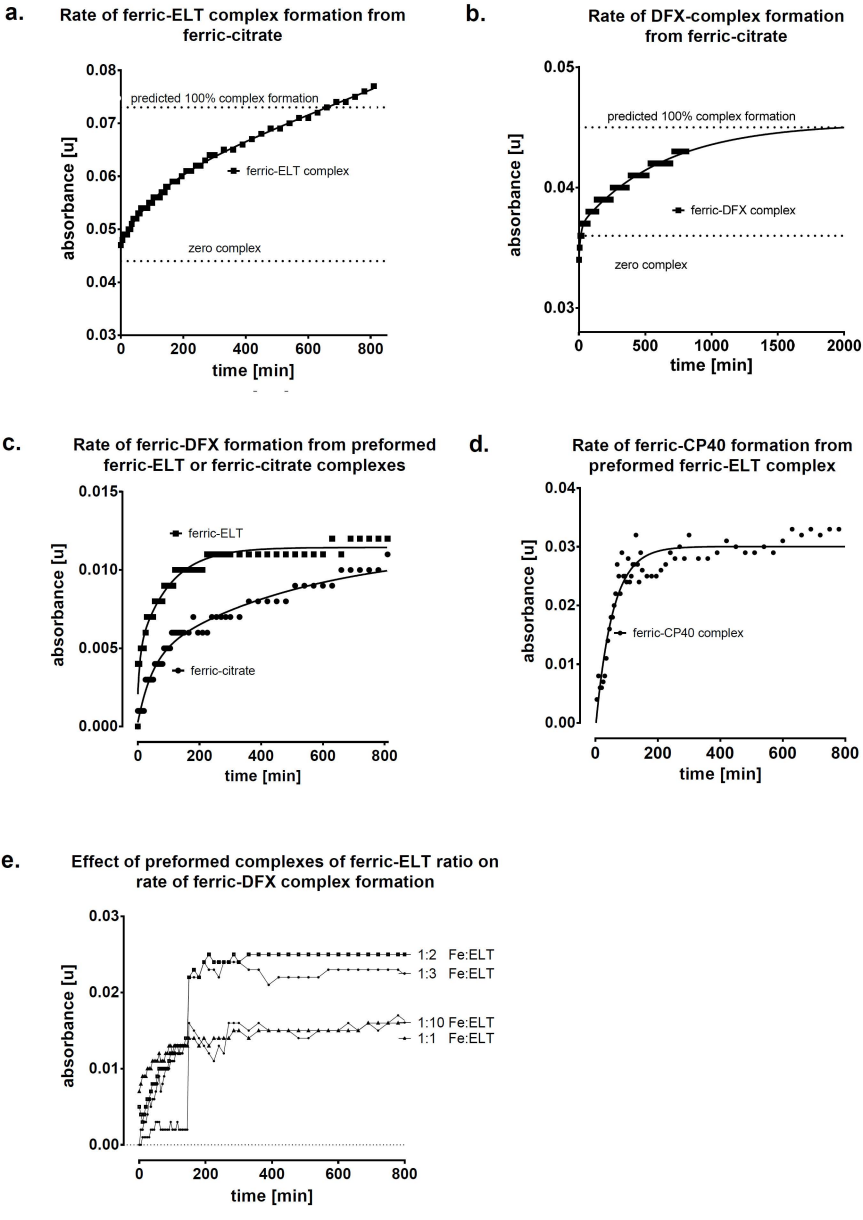
a.
Rate of ferric-ELT complex formation from ferric-citrate
predicted 100% complex formation
ferric-ELT complex
zero complex
absorbance [u]
time [min]
b.
Rate of DFX-complex formation from ferric-citrate
predicted 100% complex formation
ferric-DFX complex
zero complex
absorbance [u]
time [min]
c.
Rate of ferric-DFX formation from preformed ferric-ELT or ferric-citrate complexes
ferric-ELT
ferric-citrate
absorbance [u]
time [min]
d.
Rate of ferric-CP40 formation from preformed ferric-ELT complex
ferric-CP40 complex
absorbance [u]
time [min]
e.
Effect of preformed complexes of ferric-ELT ratio on rate of ferric-DFX complex formation
1:2 Fe:ELT
1:3 Fe:ELT
1:10 Fe:ELT
1:1 Fe:ELT
absorbance [u]
time [min]

Figure 5

a. Cellular uptake of ELT iron complexes

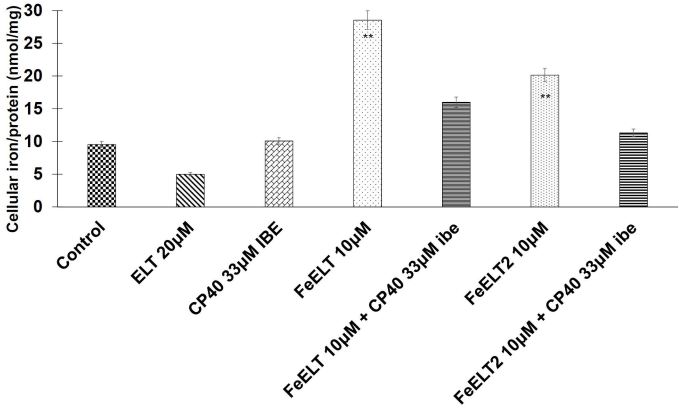

b. Cellular uptake of DFX iron complexes

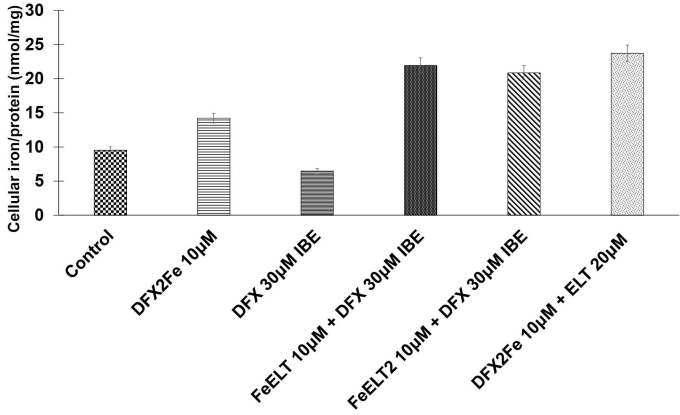

c. The FeELT – Iron Chelator Shuttle Model

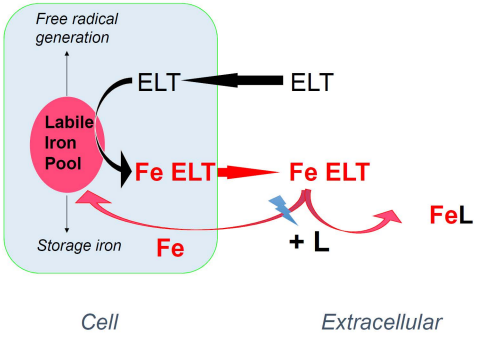

Prepublished online September 1, 2017;
doi:10.1182/blood-2016-10-740241

Eltrombopag: a powerful chelator of cellular or extracellular iron(III) alone or combined with a second chelator

Evangelia Vlachodimitropoulou, Yu-Lin Chen, Maciej Garbowski, Pimpisid Koonyosying, Bethan Psaila, Martha Sola-Visner, Nichola Cooper, Robert Hider and John Porter

Blood (print ISSN 0006-4971, online ISSN 1528-0020), is published weekly by the American Society of Hematology, 2021 L St, NW, Suite 900, Washington DC 20036.